Application of Analytical Expressions for Retarded-Time Potentials in Analyzing the Transient Scattering by Dielectric Objects

Xuezhe Tian, *Student Member, IEEE*, Gaobiao Xiao, *Member, IEEE*, and Shang Xiang, *Student Member, IEEE*

***Abstract*—Application of analytical formulas for the retarded-time potentials in Müller- and PMCHWT-type time-domain integral equations (TDIEs) is presented. The impulsively excited scalar and vector potentials are evaluated in closed form, and the coupling coefficients can be calculated with high accuracy. Examples of transient analysis of the electromagnetic scattering from dielectric objects are provided and solved with marching-on-in-time (MOT) method. Numerical results show that solutions for Müller-type MOT TDIE are always stable if the coupling coefficients are accurately evaluated, while the PMCHWT type usually suffers from the dc instability.**

***Index Terms*—Marching-on-in-time (MOT), Müller equation, PMCHWT, time-domain integral equation, transient electromagnetic scattering.**

I. Introduction

TIME-DOMAIN integral equations (TDIEs) remain appealing to researchers for their advantages in analyzing transient radiation and scattering problems in large-scale and complex structures, as well as in wideband applications [1], [2]. To remedy the late time instabilities, techniques like averaging [3], implicit time-stepping method [4], smooth temporal basis functions [5], precise integration schemes [6]–[12], and Calderón preconditioning [13] are proposed.

Many research results have shown that high precision of the coupling coefficients between the bases in marching-on-in-time (MOT) method often provides substantial stabilizing effects. Closed-form formulas for calculating the retarded-time potentials in electric field integral equation (EFIE) and magnetic field integral equation (MFIE) are derived [7], [8]. Applications of these formulas in different TDIEs for conductors are detailed in [9]. When evaluating the potentials in MFIE, spatial derivatives of the arc length and its bisecting vector function need to be calculated, and their singular behaviors should be carefully handled [10].

In this letter, analytical expressions in [7] and [8] with some modifications are applied in the transient analysis of dielectric objects. Compared to the previous expressions, they are more concise and compact. Moreover, it is shown that only two kinds of impulsive retarded-time potentials are needed to implement the PMCHWT- and Müller-based TDIE solvers for dielectric objects [11], [14]. The spatial derivative on the Delta impulsive potentials in [8] is avoided, and the original singularities are directly removed or extracted.

Manuscript received June 08, 2014; accepted June 24, 2014. Date of publication July 09, 2014; date of current version July 18, 2014. This work was supported by the SAST Foundation 2013 and the National Science Foundation of China under Grant 61234001.

The authors are with Shanghai Jiao Tong University, Shanghai 200240, China (e-mail: smarter@sjtu.edu.cn).

Color versions of one or more of the figures in this letter are available online at http://ieeexplore.ieee.org.

Digital Object Identifier 10.1109/LAWP.2014.2336471

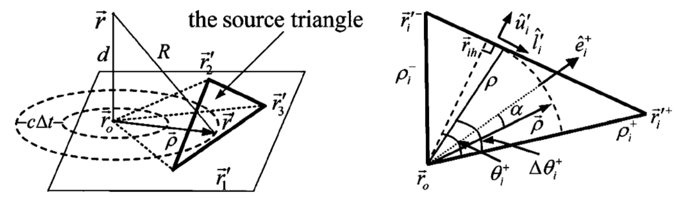

(a) (b)

Fig. 1. Geometric parameter definitions. (a) Observation point $\vec{r}$ projecting on the source triangle. (b) Parameters for one subtriangle.

II. Analytical Expressions for Retarded-Time Potentials in Müller and PMCHWT Equations

A. Analytical Expressions for the Retarded-Time Potentials

There are two basic kinds of impulsively retarded-time potentials in the TDIEs, the scalar one and the vector one, which are defined as follows [7]:

$$\Gamma_n(\vec{r},t) = \int_{S_n} \frac{\delta(t-R/c)}{R}\, dS' \tag{1}$$

$$\vec{\mathbf{\Gamma}}_n(\vec{r},t) = \int_{S_n} \frac{\delta(t-R/c)}{R}(\vec{r}' - \vec{r}_o)\, dS' \tag{2}$$

where $\vec{r}_o$ is the projection of the observation point $\vec{r}$ on the source triangle plane, and $R = |\vec{r} - \vec{r}'|$ represents the distance between the source and field points. S_n is one triangle patch of the nth RWG basis that models the object. c is the speed of light in free space.

In [7]–[9], closed-form expressions for Γ_n and $\vec{\mathbf{\Gamma}}_n$ are provided. Here, we present them in a more compact way. Geometric parameters in the new expressions are depicted in Fig. 1(a) and (b). $\vec{r'}_1$, $\vec{r'}_2$, and $\vec{r'}_3$ are the vertices of a source triangle. The distance between the field point $\vec{r}$ and the source triangle plane is denoted by $d = (\vec{r} - \vec{r'}_1)\cdot\hat{n}'$, in which $\hat{n}'$ is the unit normal vector of the source triangle. $\vec{\rho} = \vec{r'} - \vec{r}_o$ is the local in-plane coordinates. For edge i of the source triangle, $\hat{u}_i'$ is its outward unit normal vector, and $\hat{l'}_i$ is the unit tangential vector, pointing from $\vec{r'}_i^-$ to $\vec{r'}_i^+$. They are subject to $\hat{u}_i' = \hat{l'}_i \times \hat{n}'$.

The source triangle is divided into three subtriangles with a common node $\vec{r}_o$, as is shown in Fig. 1(a). Then, the integration is carried out on each subtriangle respectively. We can see that Γ_n and $\vec{\boldsymbol{\Gamma}}_n$ are respectively related to the central angle and bisecting vector of the intersecting arcs. Through the vertex coordinates of the RWG patches and some sign symbols, the integration of (1) and (2) can be finally expressed by

$$\Gamma_n(\vec{r},t) = c\sum_{i=1}^{3}\operatorname{sign}(h_i)\left(\sigma_i^+\Delta\theta_i^+ - \sigma_i^-\Delta\theta_i^-\right) \tag{3}$$

$$\vec{\boldsymbol{\Gamma}}_n(\vec{\boldsymbol{r}},t) = 2\rho c\sum_{i=1}^{3}\operatorname{sign}(h_i) \times\left(\sigma_i^+\hat{e}_i^+\sin\frac{\Delta\theta_i^+}{2} - \sigma_i^-\hat{e}_i^-\sin\frac{\Delta\theta_i^-}{2}\right) \tag{4}$$

in which

$$\rho = |\vec{\rho}| = \sqrt{(ct)^2 - d^2},\ \rho_i^{\pm} = |\vec{r'}_i^{\pm} - \vec{r}_o|$$
$$h_i = \left(\vec{r'}_i^{+} - \vec{r}\right)\cdot\hat{u}'_i,\ \sigma_i^{\pm} = \operatorname{sign}\left[\left(\vec{r'}_i^{\pm} - \vec{r}\right)\cdot\hat{l}'_i\right]$$
$$\Delta\theta_i^{\pm} = \begin{cases}\cos^{-1}\left(\dfrac{|h_i|}{\rho_i^{\pm}}\right), & \rho\le|h_i|\\[2mm] \cos^{-1}\left(\dfrac{|h_i|}{\rho_i^{\pm}}\right) - \cos^{-1}\left(\dfrac{|h_i|}{\rho}\right), & |h_i|<\rho<\rho_i^{\pm}\\[2mm] 0, & \rho\ge\rho_i^{\pm}\end{cases} \tag{5}$$

$$\hat{e}_i^{\pm} = \operatorname{sign}(h_i)\cos\left(\theta_i^{\pm} - \frac{\Delta\theta_i^{\pm}}{2}\right)\hat{u}'_i + \sigma_i^{\pm}\sin\left(\theta_i^{\pm} - \frac{\Delta\theta_i^{\pm}}{2}\right)\hat{l}'_i. \tag{6}$$

The above-listed formulas can be programmed without the necessity to calculate the intersecting points. The geometric relationships between the concentric time spheres and the source triangle can be judged automatically. Careful examination of (3)–(6) shows that there is no apparent singularity evolved.

B. Müller and PMCHWT Equation

Consider a dielectric body bounded by surface S residing in a homogeneous background. The exterior region and dielectric region are denoted as v_1 and v_2, respectively. Their permittivity and permeability are ε_v, μ_v ($v = 1, 2$). The Müller and PMCHWT equations can be expressed in a uniform way

$$\begin{bmatrix}\mathcal{S}_{11} & \mathcal{S}_{12}\\ \mathcal{S}_{21} & \mathcal{S}_{22}\end{bmatrix}\begin{bmatrix}\eta_1\vec{J}\\ \vec{M}\end{bmatrix} = \begin{bmatrix}\hat{n}\times\vec{E}_1^{inc}(\vec{r},t)\\ \hat{n}\times\eta_1\vec{H}_1^{inc}(\vec{r},t)\end{bmatrix} \tag{7}$$

where

$$\mathcal{S}_{11} = -\frac{1}{\eta_1}\left[\mu_1\mathcal{L}_1(\vec{J}) - \alpha\mu_2\mathcal{L}_2(\vec{J})\right] \tag{8}$$

$$\mathcal{S}_{12} = -(1+\alpha)\frac{\mathcal{I}}{2} + [\mathcal{K}_1(\vec{M}) - \alpha\mathcal{K}_2(\vec{M})] \tag{9}$$

$$\mathcal{S}_{21} = (1+\beta)\frac{\mathcal{I}}{2} + [-\mathcal{K}_1(\vec{J}) + \beta\mathcal{K}_2(\vec{J})] \tag{10}$$

$$\mathcal{S}_{22} = -\eta_1[\varepsilon_1\mathcal{L}_1(\vec{M}) - \beta\varepsilon_2\mathcal{L}_2(\vec{M})]. \tag{11}$$

In (7), $\hat{n}$ denotes unit norm vector of the field triangle, and the wave impedance η_1 in region-1 is used to equalize the equation. $\mathcal{I}$ is the identity operator, and $\mathcal{L}$ and $\mathcal{K}$ are the electric and magnetic integral operators, respectively, which are expressed as [11, Eq. (3)]. When $\alpha = \beta = -1$, we get the PMCHWT, and when $\beta = \mu_2/\mu_1$, $\alpha = \varepsilon_2/\varepsilon_1$, Müller formulation is obtained. It is known that PMCHWT is a Volterra integral equation of the first kind and Müller is of the second kind.

In the MOT procedure, the electric and magnetic currents are approximated as

$$\vec{J}(\vec{r},t) = \sum_{n=1}^{N_e}\sum_{k=1}^{N_t} I_{n,k}T_k(t)\vec{f}_n(\vec{r}) \tag{12}$$

$$\vec{M}(\vec{r},t) = \sum_{n=1}^{N_e}\sum_{k=1}^{N_t} M_{n,k}T_k(t)\vec{f}_n(\vec{r}) \tag{13}$$

where N_e is the number of spatial bases $\vec{f}_n(\vec{r})$ and N_t is the total temporal bases $T_k(t)$. Assume that the surface of the object is discretized by triangular patches, $\vec{f}_n(\vec{r})$ is chosen as the RWG basis function. For the temporal basis, we use the Lagrange polynomial function in [11, Eq. (6)].

Applying Galerkin's test to (7) for spatial variables and point testing for temporal variables yields the MOT schemes

$$\begin{bmatrix}Z_{11,0} & Z_{12,0}\\ Z_{21,0} & Z_{22,0}\end{bmatrix}\begin{bmatrix}I_j\\ M_j\end{bmatrix} = \begin{bmatrix}V_j^E\\ V_j^H\end{bmatrix} - \sum_{k=1}^{j-1}\begin{bmatrix}Z_{11,k} & Z_{12,k}\\ Z_{21,k} & Z_{22,k}\end{bmatrix}\begin{bmatrix}I_{j-k}\\ M_{j-k}\end{bmatrix}. \tag{14}$$

To render a well-conditioned equation, the Müller equation is tested with $\vec{f}_m(\vec{r})$, while the PMCHWT equation is tested with $\hat{n}\times\vec{f}_m(\vec{r})$. To avoid the temporal integration, we take the temporal derivative of the PMCHWT.

The operators of PMCHWT are tested with the same scheme like that in the combined field integral equation (CFIE)-based TDIEs in [9], so we only detail the differences in the Müller formulation. Only the test for the electric currents is discussed. The testing integral for the time derivative of the vector potential is very similar to that in [8], so only two kinds of testing integration need to be detailed

$$\langle\vec{f}_m(\vec{r}), -\hat{n}\times\nabla\Phi_v(\vec{r},t_k)\rangle \tag{15}$$

$$\left\langle\vec{f}_m(\vec{r}), \frac{1}{\mu_v}\hat{n}\times[P.V.\nabla\times\vec{A}_v(\vec{r},t_k)]\right\rangle. \tag{16}$$

$P.V.$ here represents the Cauchy principal value [10], and $\langle\cdot\rangle$ represents the inner product. $\vec{A}$ and Φ are the magnetic vector potential and electric scalar potential due to the electric currents (see [7, Eqs. (2) and (3)]). For (15) and (16), we only discuss the coupling between the two positive triangles S_m and S_n of the mth and nth RWGs.

For (15), we move the gradient operator from the Green's function into the testing function. By applying the Gauss divergence theorem, it can be further transformed into (see [15, Eq. (23)])

$$\langle\vec{f}_m(\vec{r}), -\hat{n}\times\nabla\Phi_v(\vec{r},t_k)\rangle = -\frac{1}{4\pi\varepsilon_v}\oint_{C_m}\hat{u}\cdot\hat{n}\times\vec{f}_m(\vec{r}) \times\int_{S_n}\frac{\partial_t^{-1}[\nabla'\cdot\vec{J}(\vec{r'},\tau_v)]}{R}\,dS'\,dl. \tag{17}$$

Here, C_m is the contour of S_m, and $\hat{u}$ is the in-plane outer unit norm vector of C_m. We use ∂_t^{-1} and ∂_t to represent the time integral and derivative, respectively. Then, (15) can be finally expressed as

$$Q_{mn}(t) * \partial_t^{-1} T(t)\big|_{t=t_k} \tag{18}$$

in which "$*$" means temporal convolution and

$$Q_{mn}(t) = -\frac{l_n}{4\pi\varepsilon_v A_n} \oint_{C_m} \hat{u}\cdot\hat{n}\times\vec{f}_m(\vec{r})\Gamma_{v,n}(\vec{r},t)\,dl. \tag{19}$$

In (19), l_n is the edge length of the nth RWG, and A_n is the area of S_n. Since $\Gamma_{v,n}(\vec{r},t)$ can be analytically evaluated, it is clear to see that no explicit singularity arises in (19).

Next, (16) can be written as

$$\left\langle \vec{f}_m(\vec{r}), \frac{1}{\mu_v}\hat{n}\times[P.V.\nabla\times\vec{A}_v(\vec{r},t_k)]\right\rangle = -\frac{1}{4\pi}\int_{S_m}\left[\begin{matrix}\hat{n}\times\vec{f}_m(\vec{r})\\ \cdot\int_{S_n}\left(\frac{1}{R^3}+\frac{1}{c_v R^2}\partial_t\right)\vec{J}(\vec{r}',\tau_v)\times\vec{R}\,dS'\end{matrix}\right]dS. \tag{20}$$

In this way, the gradient operation over Delta function in (16) is transformed into the temporal differentiation on the current, avoiding evaluation of surface integrals containing the spatial derivative of Delta function. Formula (16) can be finally cast into

$$D_{mn}(t) * \partial_t T(t)\big|_{t=t_k} + \frac{D_{mn}(t)}{t} * T(t)\Big|_{t=t_k} \tag{21}$$

in which

$$D_{mn}(t) = -\frac{l_n}{8\pi A_n} \times \int_{S_m}\left\{\begin{matrix}\hat{n}\times\vec{f}_m(\vec{r})\cdot\Big[(\vec{r}_o-\vec{r}_n)\times\hat{n}'d\frac{\Gamma_{v,n}(\vec{r},t)}{c_v(c_v t)}\\ +(\vec{r}_n-\vec{r}_o-\hat{n}'d)\times\frac{\mathbf{\Gamma}_{v,n}(\vec{r},t)}{c_v(c_v t)}\Big]\end{matrix}\right\}dS. \tag{22}$$

In (22), $\vec{r}_n$ is the free vertex of S_n. Note that (16) represents the Cauchy principle integration. The singularities in (21) and (22) at $t=0$ have already been extracted and handled in the residue self-term $\mathcal{I}$.

The singularity in the counterpart of (17) in the PMCHWT equation can be canceled using a vector identity as specified in [9]. Singularity in the counterpart of (20) in the PMCHWT equation can be similarly processed by singularity extraction.

C. Implementation of the Temporal Convolution

The convolution between the time basis function and impulsive potentials can be generally expressed by

$$F(t)*\Lambda(t) = \frac{1}{c_v}\int_{R_{\min}}^{R_{\max}} \Lambda(R/c_v)F(t-R/c_v)\,dR \tag{23}$$

in which $F(t)$ can be $T(t)$, $\partial_t T(t)$, or $\partial_t^{-1}T(t)$. $\Lambda(t)$ is one kind of integral potential. Here, the spatial testing integral is performed first and then convoluted with the temporal basis, as is in [9]. The temporal convolution is numerically implemented. It is computationally efficient and also amenable for different temporal basis. Moreover, to avoid the discontinuities in the derivatives of the temporal basis, $\Lambda(R)$ is first divided into intervals whose span is $\Delta R = c_v\Delta t$, and then N_{s} points are sampled in each interval. N_{s} is adaptively selected for the integral according to the support of $\Lambda(R)$ and ΔR.

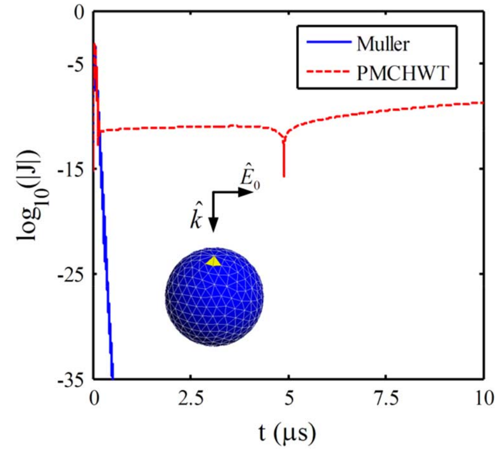

Fig. 2. Electric current of the observed RWG on the sphere.

III. Numerical Results

Modulated Gaussian plane wave is chosen to be the incident field, which can be expressed in the following form:

$$\vec{E}^i(\vec{r},t) = \hat{p}e^{-\gamma^2}\cos(2\pi f_0\tau) \tag{24}$$

where $\gamma = (\tau - t_p)/(\sqrt{2}\sigma)$, $\tau = t-(\vec{r}\cdot\hat{k})/c$, $\sigma = 3/(2\pi f_{bw})$, and $t_p = 8\sigma$. $\hat{p}$ is the polarization, and $\hat{k}$ is the direction of propagation. In all the numerical experiments, we set $\hat{p} = -\hat{x}$ and $\hat{k} = -\hat{z}$. To evaluate the matrix elements, the outer spatial integrations are carried out using 25-points Gauss quadrature for surface integrals and 10-points Gauss–Legendre rule for line integrals. $N_{\mathrm{s}} = 10$ for the temporal convolution. Third-order temporal basis function is adopted. The oversampling factor χ_{o} is introduced to determine the time-step $\Delta t = 1/(2\chi_{\mathrm{o}} f_{\max})$. The equations are solved directly using LU decomposition.

A. Dielectric Sphere

In the first example, transient scattering from a dielectric sphere with radius 1 m, $\varepsilon_{\mathrm{r}} = 2.0$, and $\mu_{\mathrm{r}} = 1.0$ is analyzed. The surface mesh is composed of 216 triangles, forming 324 RWGs. $f_0 = 130$ MHz, and $f_{\mathrm{bw}} = 70$ MHz. The time-step is 0.5 ns, with $\chi_{\mathrm{o}} = 5$.

Current coefficients of the highlighted RWG basis in 0–10 μs are depicted in Fig. 2. As the figure shows, the current decays exponentially after the incident vanishes for the Müller-based solver, while the solution of PMCHWT has a slowly growing magnitude, owing to the dc instability described in [13] and [16]. There are no resonance instabilities in both of the solvers, even when the lowest resonant frequency (131 MHz) of the unit spherical cavity is included in the incident field. The eigenvalues of their companion matrix [13] are plotted in Fig. 3. We can see that all eigenvalues of the Müller equation

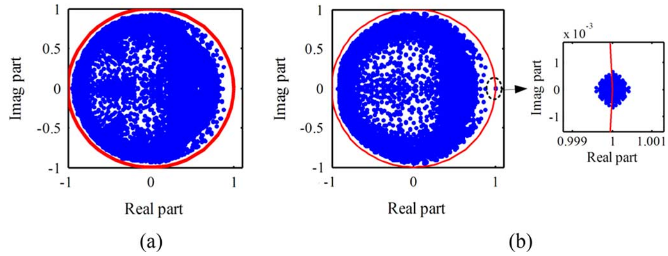

Fig. 3. Eigenvalues for the dielectric sphere of the MOT TDIEs: (a) Müller type; (b) PMCHWT type.

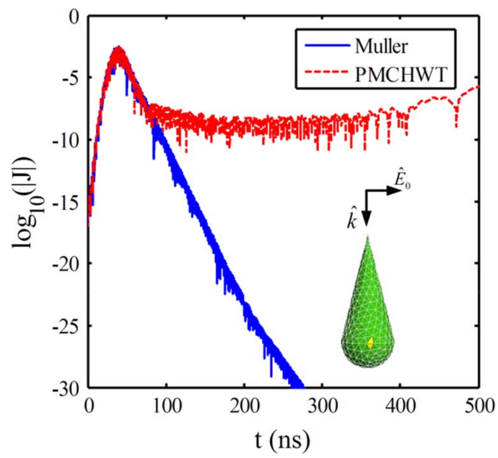

Fig. 4. Electric current of the conesphere at the observation RWG.

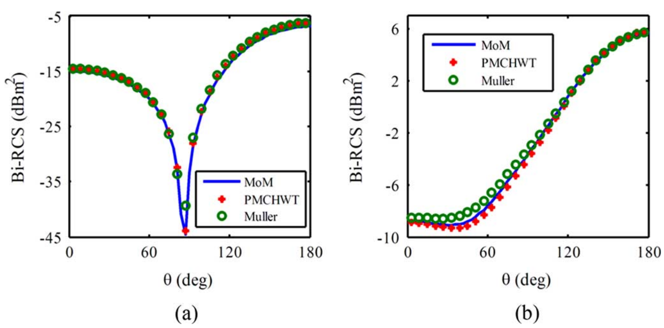

Fig. 5. Comparison of bistatic RCS ($\varphi = 0$) obtained by MOT and MoM codes for the cone-sphere at (a) 150 and (b) 250 MHz.

are distributed inside the unit circle, while there is a cluster of eigenvalues around $(1+0i)$ in the PMCHWT equation.

B. Cone-Sphere

Next, transient scattering from a cone-sphere with relative permittivity 4.0 is analyzed. The radius of the base of the cone is 0.25 m, and the height is 1.0 m. The surface is modeled by 879 RWGs. The incident field is characterized by $f_0 = 200$ MHz, $f_{\rm bw} = 100$ MHz. The time-step is 1/6 ns, with $\chi_{\rm o} = 10$.

Electric currents are shown in Fig. 4, for 3000 time-steps. Early time solutions of the Müller and the PMCHWT equations agree well with each other. In the late time, solutions of the Müller are exponentially stable, but the dc instabilities show up again in solutions of the PMCHWT equation. In Fig. 5, RCS data sets by the MOT solvers are compared to that by the PMCHWT-based method-of-moments (MoM) solver at 150 and 250 MHz, which clearly demonstrate the accuracy of the MOT solvers.

IV. Conclusion

Compact closed-form expressions for time-domain potential integrals are applied for accurately evaluating mutual coupling coefficients between RWG elements. Müller and PMCHWT equations incorporated with these formulas are implemented for analyzing transient scattering of homogeneous dielectric objects. Numerical results show that if the matrix entries are accurately evaluated, Müller-type MOT solver is always stable, while its solution decays exponentially. However, the PMCHWT type is prone to dc instabilities.

References

[1] S. M. Rao and D. R. Wilton, "Transient scattering by conducting surfaces of arbitrary shape," *IEEE Trans. Antennas Propag.*, vol. 39, no. 1, pp. 56–61, Jan. 1991.

[2] T. K. Sarkar, W. Lee, and S. M. Rao, "Analysis of transient scattering from composite arbitrarily shaped complex structures," *IEEE Trans. Antennas Propag.*, vol. 48, no. 10, pp. 1625–1634, Oct. 2000.

[3] A. Sadigh and E. Arvas, "Treating the instabilities in marching-on-in-time method from a different perspective," *IEEE Trans. Antennas Propag.*, vol. 41, no. 12, pp. 1695–1702, Dec. 1993.

[4] S. M. Rao and T. K. Sarkar, "Implicit solution of time domain integral equations for arbitrarily shaped dielectric bodies," *Microw. Opt. Technol. Lett.*, vol. 21, no. 3, pp. 201–205, May 1999.

[5] D. S. Weile *et al.*, "A novel scheme for the solution of the time-domain integral equations of electromagnetics," *IEEE Trans. Antennas Propag.*, vol. 52, no. 1, pp. 283–295, Jan. 2004.

[6] J. Pingenot, S. Chakraborty, and V. Jandhyala, "Polar integration for exact space-time quadrature in time-domain integral equations," *IEEE Trans. Antennas Propag.*, vol. 54, no. 10, pp. 3037–3042, Oct. 2006.

[7] A. C. Yucel and A. A. Ergin, "Exact evaluation of retarded-time potential integrals for the RWG bases," *IEEE Trans. Antennas Propag.*, vol. 54, no. 5, pp. 1496–1502, May 2006.

[8] H. A. Ülkü and A. A. Ergin, "Analytical evaluation of transient magnetic fields due to RWG current bases," *IEEE Trans. Antennas Propag.*, vol. 55, no. 12, pp. 3565–3575, Dec. 2007.

[9] H. A. Ülkü and A. A. Ergin, "Application of analytical retarded-time potential expressions to the solution of time domain integral equations," *IEEE Trans. Antennas Propag.*, vol. 59, no. 11, pp. 4123–4131, Nov. 2011.

[10] H. A. Ülkü and A. A. Ergin, "On the singularity of the closed-form expression of the magnetic field in time domain," *IEEE Trans. Antennas Propag.*, vol. 59, no. 2, pp. 691–694, Feb. 2011.

[11] B. Shanker, M. Lu, J. Yuan, and E. Michielssen, "Time domain integral equation analysis of scattering from composite bodies via exact evaluation of radiation fields," *IEEE Trans. Antennas Propag.*, vol. 57, no. 5, pp. 1506–1520, May 2009.

[12] A. J. Pray, N. V. Nair, and B. Shanker, "Stability properties of the time domain electric field integral equation using a separable approximation for the convolution with the retarded potential," *IEEE Trans. Antennas Propag.*, vol. 60, no. 8, pp. 3772–3781, Aug. 2012.

[13] F. P. Andriulli, K. Cools, F. Olyslager, and E. Michielssen, "Time domain Calderón identities and their application to the integral equation analysis of scattering by PEC objects Part II: Stability," *IEEE Trans. Antennas Propag.*, vol. 57, no. 8, pp. 2365–2375, Aug. 2009.

[14] P. Ylä-Oijala and M. Taskinen, "Well-conditioned Müller formulation for electromagnetic scattering by dielectric objects," *IEEE Trans. Antennas Propag.*, vol. 53, no. 10, pp. 3316–3323, Oct. 2005.

[15] P. Ylä-Oijala and M. Taskinen, "Calculation of CFIE impedance matrix elements with RWG and n × RWG functions," *IEEE Trans. Antennas Propag.*, vol. 51, no. 8, pp. 1837–1846, Aug. 2003.

[16] G. Pisharody and D. S. Weile, "Electromagnetic scattering from homogeneous dielectric bodies using time-domain integral equations," *IEEE Trans. Antennas Propag.*, vol. 54, no. 2, pp. 687–697, Feb. 2006.